

# A further analysis of $\Theta^+$ production in $\gamma + D \rightarrow \Lambda + n + K^+$ reaction

V. Guzey\*

*Institut für Theoretische Physik II,*

*Ruhr-Universität Bochum, D-44780 Bochum, Germany*

## Abstract

We analyse  $\Theta^+$  production in the  $\gamma + D \rightarrow \Lambda + n + K^+$  reaction and study the dependence of the  $\gamma + D \rightarrow \Lambda + n + K^+$  differential cross section on the  $nK^+$  invariant mass and on the momentum of the final neutron  $p_n$ . We examine the important role of the interference between the signal and background contributions to the  $\gamma + D \rightarrow \Lambda + n + K^+$  amplitude in the extraction of the  $\Theta^+$  signal from the  $\gamma + D \rightarrow \Lambda + n + K^+$  cross section. We demonstrate that as a result of the cancellation between the interference and signal contributions, the  $\Theta^+$  signal almost completely washes out after the integration over  $p_n$ . This is consistent with the CLAS conclusion that no statistically significant structures in the analysis of the  $\gamma + D \rightarrow \Lambda + n + K^+$  reaction were observed. Therefore, there is no disagreement between the theory and the experiment and the CLAS result does not refute the existence of the  $\Theta^+$ .

PACS numbers: 13.60.Rj, 14.20.Jn, 25.20.Lj

arXiv:hep-ph/0608129v1 11 Aug 2006

---

\*Electronic address: vadim.guzey@tp2.rub.de

## I. INTRODUCTION

Three and a half years have passed since the announcement of the discovery of an exotic pentaquark baryon, the  $\Theta^+$ , by the LEPS collaboration [1]. This announcement has renewed the interest and enthusiasm in hadron spectroscopy: The original LEPS publication was followed by tens of measurements aiming to confirm or refute the LEPS result and by hundreds of theoretical analyses of properties of the  $\Theta^+$ , possible mechanisms of its production and many other related issues, see [2] for a review of the experimental situation in 2005. Over the time, the experimental status of the  $\Theta^+$  has changed dramatically: Many initial experiments confirming the  $\Theta^+$  were followed by mostly negative results on the  $\Theta^+$  search. At the moment, the only experiment, which officially confirmed its own initial claim of the  $\Theta^+$  discovery, is the measurement of the  $K^+Xe \rightarrow K^0pXe'$  reaction by DIANA collaboration [3]. In summary, if the  $\Theta^+$  exists, its exotic properties make it very difficult to unambiguously establish its existence. All indirect measurements used so far proved to be inefficient and marred by significant experimental and theoretical uncertainties. Most likely, only future dedicated experiments using kaon beams (note the still standing positive result of DIANA [3] using the kaon beam) will be able to answer the question whether the  $\Theta^+$  exists or not.

The properties of the  $\Theta^+$  and other members of the antidecuplet, the flavor SU(3) multiplet containing the  $\Theta^+$ , were first predicted in the chiral quark soliton model by Diakonov, Petrov and Polyakov in 1997 [4]. The predicted positive strangeness of the  $\Theta^+$  indicates that in the language of the quark model, the  $\Theta^+$  has the minimal structure  $uudd\bar{s}$ , i.e. it is an exotic pentaquark baryon. Another remarkable property of the  $\Theta^+$ , which makes it "doubly exotic", is the predicted small total width of the  $\Theta^+$ ,  $\Gamma_\Theta < 15$  MeV [4]. In reality, the total width is possibly even smaller: The recent theoretical estimates range between 2-5 MeV [5, 6] and 1 MeV [7, 8, 9]. The experimental upper bound on  $\Gamma_\Theta$  is usually given by the spectrometer resolution, which is of the order of 5-10 MeV. However, in some cases, more stringent constraints can be derived. For instance, the recent DIANA analysis reports  $\Gamma_\Theta = 0.36 \pm 0.11$  MeV [3].

The small value of  $\Gamma_\Theta$ , the unknown mechanism of production of the  $\Theta^+$  (the necessity to impose various cuts on the data in order to enhance the signal, which dramatically reduces the statistics) and generally rather small cross sections of the  $\Theta$  production (at the

nanobarn level) make all analyses attempting to extract the  $\Theta^+$  signal model-dependent and inconclusive. Naturally, this does not necessarily mean that the  $\Theta^+$  does not exist. The majority of the experiments simply might not have enough sensitivity (enough statistics) to observe the elusive  $\Theta^+$ .

In this work, we consider protoproduction of the  $\Theta^+$  on deuterium in the reaction  $\gamma + D \rightarrow \Lambda + n + K^+$ . While we comprehensively studied this reaction earlier [10], the very recent CLAS measurement [11] compels us to perform further studies. In particular, in order to make a better comparison between our theoretical predictions and the experimental results, we analyse in detail the differential cross section of the  $\gamma + D \rightarrow \Lambda + n + K^+$  process as function of the  $nK^+$  invariant mass and of the momentum of the final neutron,  $p_n$ . We discuss the important role of the interference between the signal and background and examine its  $p_n$ -dependence. We demonstrate that after integrating over  $p_n$  and the photon energy as was done in the CLAS analysis [11], one does not expect any significant structures associated with the  $\Theta^+$  in the  $\gamma + D \rightarrow \Lambda + n + K^+$  cross section. This is consistent with the CLAS analysis, which reports no statistically significant structures [11]. Therefore, there is no disagreement between the theory and the experiment. The CLAS result does not refute the existence of the  $\Theta^+$ .

## II. INTERFERENCE BETWEEN THE BACKGROUND AND THE SIGNAL AND THE SIZE OF THE $\Theta^+$ SIGNAL

In order to make our presentation self-contained, we shall repeat in detail the derivation of key expressions from our original analysis [10].

### A. The signal amplitude

We assume that the dominant mechanism of the  $\Theta^+$  production in the reaction  $\gamma + D \rightarrow \Lambda + n + K^+$  is given by the Feynman graphs presented in Fig. 1. The corresponding scattering amplitude reads

$$\begin{aligned} \mathcal{A}_S = & -i \int \frac{d^4k}{(2\pi)^4} \bar{u}(p_n) \hat{\Gamma}_\Theta \frac{\hat{p}_\Theta + M_\Theta}{p_\Theta^2 - M_\Theta^2 + i\Gamma_\Theta M_\Theta} \hat{\Gamma}_\Theta \\ & \times \frac{\hat{k} + m_N}{k^2 - m_N^2 + i0} \frac{1}{(p_\Theta - k)^2 - m_K^2 + i0} \bar{u}(p_\Lambda) \hat{\Gamma}_\Lambda^{p+n} \frac{\hat{p}_D - \hat{k} + m_N}{(p_D - k)^2 - m_N^2 + i0} \hat{\Gamma}_D, \quad (1) \end{aligned}$$

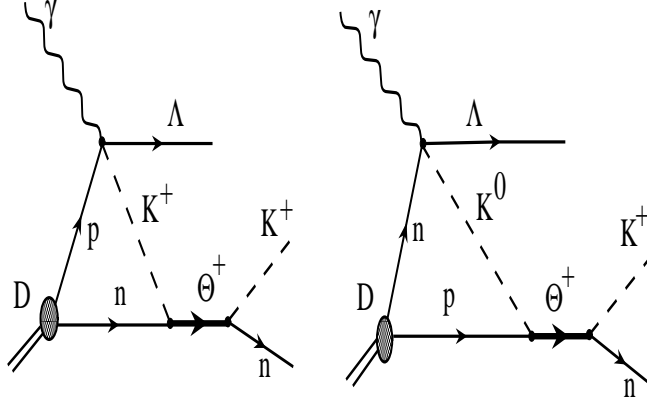


FIG. 1: The assumed mechanism of  $\Theta^+$  production in the  $\gamma + D \rightarrow \Lambda + n + K^+$  reaction.

where  $p_n$  is the momentum of the final neutron;  $p_\Lambda$  is the momentum of the  $\Lambda$ ;  $p_\Theta$  is the momentum of the virtual  $\Theta^+$ ;  $k$  is the momentum of the spectator nucleon in the loop; the  $\hat{\Gamma}_\Theta$  vertex describes the  $\Theta^+ \rightarrow nK^+$  transition; the  $\hat{\Gamma}_\Lambda^{p+n}$  vertex describes the sum of the  $\gamma + p \rightarrow \Lambda + K^+$  and  $\gamma + n \rightarrow \Lambda + K^0$  transitions; the  $\hat{\Gamma}_D$  vertex describes the  $D \rightarrow pn$  transition. For brevity, we do not write explicitly spinor polarization indices.

The loop integration in Eq. (1) receives its dominant contribution from the integration region, when the spectator nucleon and the virtual kaon tend to be on the mass-shell. Then, the dominating imaginary part of the loop integral can be evaluated through the discontinuity of the loop integral using Cutkosky cutting rules

$$2 \text{Im} \left( i \int \frac{d^4k}{(2\pi)^4} \frac{1}{k^2 - m_N^2 + i0} \frac{1}{(p_\Theta - k)^2 - m_K^2 + i0} \right) = (2\pi i)^2 \int \frac{d^4k}{(2\pi)^4} \delta(k^2 - m_N^2) \delta((p_\Theta - k)^2 - m_K^2) \Theta(k^0) \Theta(p_\Theta^0 - k^0). \quad (2)$$

As we discussed in the Introduction,  $\Gamma_\Theta$  is very small. Hence, the signal amplitude is non-vanishing only near  $p_\Theta^2 \approx M_\Theta^2$  and one can approximately write

$$\frac{1}{p_\Theta^2 - M_\Theta^2 + i\Gamma_\Theta M_\Theta} \approx -i \frac{\Gamma_\Theta M_\Theta}{(p_\Theta^2 - M_\Theta^2)^2 + (\Gamma_\Theta M_\Theta)^2}. \quad (3)$$

Therefore, the signal scattering amplitude can be written as

$$\begin{aligned}
\mathcal{A}_S &= \int \frac{d^4k}{(2\pi)^4} \bar{u}(p_n) \hat{\Gamma}_\Theta u(p_\Theta) \bar{u}(p_\Theta) \hat{\Gamma}_\Theta u(k) \bar{u}(p_\Lambda) \hat{\Gamma}_\Lambda^{p+n} u(p_D - k) \frac{\Gamma_\Theta M_\Theta}{(p_\Theta^2 - M_\Theta^2)^2 + (\Gamma_\Theta M_\Theta)^2} \\
&\times \bar{u}(p_D - k) \bar{u}(k) \frac{\hat{\Gamma}_D}{(p_D - k)^2 - m_N^2 + i0} \delta(k^2 - m_N^2) \delta((p_\Theta - k)^2 - m_K^2) \\
&\times \Theta(k^0) \Theta(p_\Theta^0 - k^0), \tag{4}
\end{aligned}$$

where  $p_D - k$  is the momentum of the interacting nucleon in the loop. It is important to note that the resulting signal scattering amplitude has an overall plus sign. As will be shown below, this will lead to the destructive interference between the signal and the background amplitudes. In our original work [10], it was erroneously derived that the sign should be negative. However, this mistake was not important there since the role of the interference between the two amplitudes was very small in the kinematics considered in [10].

The factor  $\Gamma_\Theta M_\Theta / [(p_\Theta^2 - M_\Theta^2)^2 + (\Gamma_\Theta M_\Theta)^2]$  in Eq. (4) forces the virtual  $\Theta^+$  on its mass-shell. This means that one can neglect the off-shellness of the  $\Theta^+$  in the  $\Theta^+ \rightarrow NK$  vertex. Therefore, the corresponding factor in Eq. (4) depends only on the involved masses and  $\Gamma_\Theta$ ,

$$\bar{u}(p_n) \hat{\Gamma}_\Theta u(p_\Theta) \bar{u}(p_\Theta) \hat{\Gamma}_\Theta u(k) = \frac{8\pi M_\Theta^3 \Gamma_\Theta}{\lambda^{1/2}(M_\Theta^2, m_N^2, m_K^2)}, \tag{5}$$

where  $\lambda(x, y, z)$  is the so-called triangular kinematic function,  $\lambda(x, y, z) = (x - y - z)^2 - 4y^2 z^2$ . In the derivation of Eq. (5) we used the textbook relation between the  $1 \rightarrow 2$  decay amplitude and the corresponding decay width and the fact that  $\Gamma_{\Theta^+ \rightarrow nK^+} = (1/2)\Gamma_\Theta$ .

In the vertex describing the  $\gamma + N \rightarrow \Lambda + K$  transition in Eq. (4), the interacting nucleon is off-shell. However, since the effect of the off-shellness is small, we shall ignore it and use for the  $\gamma + N \rightarrow \Lambda + K$  scattering amplitudes their on-shell expressions [12]. Moreover, since the sensitivity of our results to the fine details of the  $\gamma + N \rightarrow \Lambda + K$  transition is not large and since the nuclear wave function suppresses the contribution of large nucleon momenta, we assume that the scattering takes place on the nucleon at rest. At this point, it is convenient to introduce the following short-hand notation

$$\bar{u}(p_\Lambda) \hat{\Gamma}_\Lambda^{p+n} u(p_D - k) = V_\Lambda^{p+n}(E_\gamma, t), \tag{6}$$

which demonstrates that the  $\gamma + N \rightarrow \Lambda + K$  amplitude depends only on the photon energy  $E_\gamma$  and  $t = (p_\gamma - p_\Lambda)^2$ .

One has to point out that the  $\gamma + p \rightarrow \Lambda + K^+$  and  $\gamma + n \rightarrow \Lambda + K^0$  scattering amplitudes, which correspond to the left and right hand side figures in Fig. 1, respectively, enter Eq. (4) with the relative plus sign. This is a consequence of the observation that only the isospin-zero part of the electromagnetic current contributes (we used that the  $\Theta^+$  has isospin zero).

Further, the  $D \rightarrow NN$  vertex  $\hat{\Gamma}_D$  in Eq. (4) can be related to the deuteron non-relativistic wave function  $\psi_D$

$$\bar{u}(p_D - k)\bar{u}(k)\frac{\hat{\Gamma}_D}{(p_D - k)^2 - m_N^2 + i0} = \sqrt{(2\pi)^3 2m_N} \psi_D(k). \quad (7)$$

This non-relativistic reduction means that we have to work in the laboratory (target rest) frame. In our work, we used the Paris deuteron wave function [13].

The two delta-functions in Eq. (4) enable one to take integrals over  $k^0$  and the angle between the vectors  $\vec{k}$  and  $\vec{p}_\Theta$  (nothing depends on the azimuthal angle, so that the integration over it simply gives  $2\pi$ ).

The resulting expression for the signal scattering amplitude has the following compact form

$$\begin{aligned} \mathcal{A}_S &= \frac{\Gamma_\Theta M_\Theta}{(M_{NK}^2 - M_\Theta^2)^2 + (\Gamma_\Theta M_\Theta)^2} V_\Lambda^{p+n}(E_\gamma, t) \frac{8\pi M_\Theta^3 \Gamma_\Theta}{\lambda^{1/2}(M_\Theta^2, m_N^2, m_K^2)} \\ &\times \frac{\sqrt{(2\pi)^3 2m_N}}{16\pi} \int dk \frac{k}{E_k} \Theta(E_\Theta - E_k) \frac{\theta(E_\gamma, t, M_{NK}^2; k)}{|\vec{p}_\Theta|} \psi_D(k), \end{aligned} \quad (8)$$

where  $M_{NK}$  is the invariant mass of the final  $nK^+$  system,  $M_{NK}^2 \equiv p_\Theta^2$ ;  $\theta(E_\gamma, t, M_{NK}^2; k)$  denotes the  $\theta$ -function remaining after the angular integration,

$$\theta(E_\gamma, t, M_{NK}^2; k) \equiv \Theta\left(-1 \leq \frac{2E_\Theta E_k + m_K^2 - m_N^2 - M_{NK}^2}{2|\vec{p}_\Theta|k} \leq 1\right). \quad (9)$$

In Eqs. (8) and (9),  $E_k = \sqrt{k^2 + m_N^2}$ ;  $p_\Theta = \sqrt{(E_\gamma - E_\Lambda)^2 - t}$ ;  $E_\Theta = \sqrt{M_{NK}^2 + (\vec{p}_\Theta)^2}$ ;  $E_\Lambda = (t + m_D^2 + 2m_D E_\gamma - M_{NK}^2)/(2m_D)$ .

## B. The background amplitude

We suppose that the main background contribution to the considered process is the  $\gamma + p \rightarrow \Lambda + K^+$  scattering on the quasi-free proton, which is depicted in Fig. 2. Note that other background reactions are also possible [14], but their contributions are suppressed in the kinematics considered in this work.

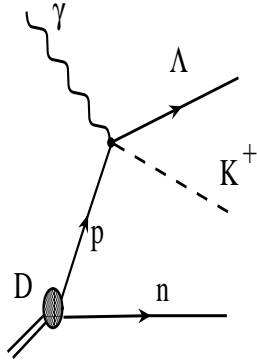


FIG. 2: The main background contribution to the  $\gamma + D \rightarrow \Lambda + n + K^+$  reaction in the kinematics considered in this work.

The background scattering amplitude corresponding to the Feynman graph in Fig. 2 reads

$$\begin{aligned} \mathcal{A}_{\text{BG}} &= -\bar{u}(p_\Lambda) \hat{\Gamma}_\Lambda^p \frac{\hat{p}_D - \hat{k} + m_N}{(p_D - k)^2 - m_N^2 + i0} \bar{u}(p_n) \hat{\Gamma}_D \\ &= -\sqrt{(2\pi)^3} 2m_N \psi_D(p_n) V_\Lambda^p(E_\gamma, t), \end{aligned} \quad (10)$$

where  $V_\Lambda^p(E_\gamma, t)$  denotes the  $\gamma + p \rightarrow \Lambda + K^+$  scattering amplitude. In the derivation of the second line of Eq. (10), we have used the conventions and approximations described in the previous subsection.

The background amplitude has an overall minus sign. Therefore, its interference with the signal amplitude is destructive. As we shall argue below, the non-observation of the  $\Theta^+$  in the CLAS measurement [11] can be partially explained by the non-trivial dependence of this interference on the momentum of the final neutron  $p_n$ .

### C. The $\gamma + D \rightarrow \Lambda + n + K^+$ differential cross section and the role of the interference between the background and the signal

We would like to study the differential cross section of the  $\gamma + D \rightarrow \Lambda + n + K^+$  reaction as a function of  $t$ ,  $p_n$  and  $M_{NK}^2$ . For this purpose, it is convenient to present the three-body

phase space of the final particles as [15]

$$R_3(\gamma D \rightarrow \Lambda n K^+) \equiv \int \frac{d^3 p_\Lambda}{2E_\Lambda} \frac{d^3 p_n}{2E_n} \frac{d^3 p_K}{2E_K} \delta^4(p_\gamma + p_D - p_\Lambda - p_n - p_K) = \int dM_{NK}^2 R_2(\gamma D \rightarrow \Lambda \Theta^+) R_2(\Theta^+ \rightarrow n K^+), \quad (11)$$

where  $R_2$  stand for the corresponding two-body phase spaces. A straightforward calculation gives [15]

$$R_2(\gamma D \rightarrow \Lambda \Theta^+) = \frac{2\pi}{4\lambda^{1/2}(s, 0, m_D^2)} dt, \\ R_2(\Theta^+ \rightarrow n K^+) = \frac{\pi}{2} \frac{p_n}{E_n} \frac{\theta(E_\gamma, t, M_{NK}^2; p_n)}{p_\Theta} dp_n, \quad (12)$$

where  $s = 2E_\gamma m_D + m_D^2$ ; the  $\theta$ -function  $\theta(E_\gamma, t, M_{NK}^2; p_n)$  is given by Eq. (9) after the replacement of the spectator nucleon momentum  $k$  by the final neutron momentum  $p_n$ .

The triple differential cross section of the  $\gamma + D \rightarrow \Lambda + n + K^+$  reaction has now the following form

$$\frac{d\sigma}{dt dp_n dM_{NK}^2} = \frac{1}{(2\pi)^5} \frac{1}{4I_D} |\mathcal{A}_{BG} + \mathcal{A}_S|^2 \frac{dR_2(\gamma D \rightarrow \Lambda \Theta^+)}{dt} \frac{dR_2(\Theta^+ \rightarrow n K^+)}{dp_n}, \quad (13)$$

where  $I_D$  is the standard flux factor evaluated for real photons impinging on the deuterium target,  $I_D = \lambda^{1/2}(s, 0, m_D^2)/2$ .

As is clear from Eq. (13), the cross section receives contributions from the background, interference between the background and the signal and the signal cross sections

$$\frac{d\sigma}{dt dp_n dM_{NK}^2} = \frac{d\sigma^{BG}}{dt dp_n dM_{NK}^2} - \frac{d\sigma^I}{dt dp_n dM_{NK}^2} + \frac{d\sigma^S}{dt dp_n dM_{NK}^2}. \quad (14)$$

Evaluating  $|\mathcal{A}_{BG} + \mathcal{A}_S|^2$  in Eq. (13), the background, interference and signal cross sections in Eq. (14) take the following form

$$\frac{d\sigma^{BG}}{dt dp_n dM_{NK}^2} = \frac{\pi}{4} m_N \frac{p_n}{E_n} |\psi_D(p_n)|^2 \frac{d\sigma_\Lambda^p}{dt} \frac{\theta(E_\gamma, t, M_{NK}^2; p_n)}{p_\Theta}, \\ \frac{d\sigma^I}{dt dp_n dM_{NK}^2} = 2\Gamma_\Theta \frac{\Gamma_\Theta M_\Theta}{(M_{NK}^2 - M_\Theta^2) + (\Gamma_\Theta M_\Theta)^2} \frac{M_\Theta^3}{\lambda^{1/2}(M_\Theta^2, m_N^2, m_K^2)} \frac{d\sigma_\Lambda^I}{dt} S_D(t, p_n), \\ \frac{d\sigma^S}{dt dp_n dM_{NK}^2} = \Gamma_\Theta \frac{\Gamma_\Theta M_\Theta}{(M_{NK}^2 - M_\Theta^2) + (\Gamma_\Theta M_\Theta)^2} \frac{M_\Theta^5}{\lambda(M_\Theta^2, m_N^2, m_K^2)} \frac{d\sigma_\Lambda^{p+n}}{dt} \\ \times \frac{p_n}{E_n} \frac{\theta(E_\gamma, t, M_{NK}^2; p_n)}{p_\Theta} S_D(t). \quad (15)$$



In this equation, the combinations of the elementary  $\gamma + N \rightarrow \Lambda + K$  cross sections are given by the following expressions

$$\begin{aligned}\frac{d\sigma_{\Lambda}^p}{dt} &= \frac{1}{64\pi(E_{\gamma}m_N)^2}|\mathcal{A}^p|^2, \\ \frac{d\sigma_{\Lambda}^I}{dt} &= \frac{1}{64\pi(E_{\gamma}m_N)^2}(\mathcal{A}^p(\mathcal{A}^p + \mathcal{A}^n)^* + (\mathcal{A}^p)^*(\mathcal{A}^p + \mathcal{A}^n)), \\ \frac{d\sigma_{\Lambda}^{p+n}}{dt} &= \frac{1}{64\pi(E_{\gamma}m_N)^2}|\mathcal{A}^p + \mathcal{A}^n|^2,\end{aligned}\tag{16}$$

where  $\mathcal{A}^p$  is the scattering amplitude of the  $\gamma + p \rightarrow \Lambda + K^+$  reaction;  $\mathcal{A}^n$  is the scattering amplitude of the  $\gamma + n \rightarrow \Lambda + K^0$  reaction [12].

Finally, the nuclear suppression factors  $S_D(t, p_n)$  and  $S_D(t)$  are defined by the following expressions

$$\begin{aligned}S_D(t, p_n) &= \left(\frac{\sqrt{(2\pi)^3 2m_N}}{16\pi}\right)^2 \\ &\times \int dk \frac{k}{E_k} \Theta(E_{\Theta} - E_k) \frac{\theta(E_{\gamma}, t, M_{NK}^2; k)}{p_{\Theta}} \frac{p_n}{E_n} \frac{\theta(E_{\gamma}, t, M_{NK}^2; p_n)}{p_{\Theta}} \rho_D(k, p_n), \\ S_D(t) &= \left(\frac{\sqrt{(2\pi)^3 2m_N}}{16\pi}\right)^2 \\ &\times \int dk dk' \frac{k}{E_k} \Theta(E_{\Theta} - E_k) \frac{\theta(E_{\gamma}, t, M_{NK}^2; k)}{p_{\Theta}} \\ &\times \frac{k'}{E_{k'}} \Theta(E_{\Theta} - E_{k'}) \frac{\theta(E_{\gamma}, t, M_{NK}^2; k')}{p_{\Theta}} \rho_D(k, k'),\end{aligned}\tag{17}$$

where  $\rho_D$  is the unpolarized deuteron density matrix, which is expressed in terms of the  $S$  and  $D$ -waves of the non-relativistic deuteron wave function

$$\begin{aligned}\rho_D(k, k') &= u(k)u(k') + w(k)w(k') \left(\frac{3}{2} \frac{(\vec{k} \cdot \vec{k}')^2}{|\vec{k}|^2 |\vec{k}'|^2} - \frac{1}{2}\right), \\ &= u(k)u(k') + w(k)w(k').\end{aligned}\tag{18}$$

The last line is a consequence of the fact that the delta-functions in the loop integral over the spectator momenta in Eq. (4) make the vectors  $\vec{k}$  and  $\vec{k}'$  collinear.

Examples of the  $d\sigma_{\Lambda}^{p+n}/dt$  and  $d\sigma_{\Lambda}^p/dt$  cross sections and the  $S(t)$  nuclear suppression factor can be found in our original publication [10] and shall not be repeated here.

In our original work [10], we mostly concentrated on the triple differential cross section  $d\sigma/(dtdp_n dM_{NK}^2)$  at large  $p_n$  ( $p_n \geq 0.3$  GeV), which is dominated by the signal contribution.

In the present work, in order to better compare our predictions to the results of the CLAS analysis [11], we concentrate on the  $t$ -integrated cross section  $d\sigma/(dp_n dM_{NK}^2)$  as a function of  $M_{NK}^2$  and  $p_n$  for  $0.1 \leq p_n \leq 0.3$  MeV. We shall also consider the  $p_n$ -integrated cross section.

Before performing any numerical calculations, it is important to qualitatively understand the behavior of  $d\sigma/(dp_n dM_{NK}^2)$ . For the values of the invariant mass of the  $nK^+$  system,  $M_{nK}$ , which is away from the expected mass of the  $\Theta^+$ ,  $M_\Theta = 1540$  MeV, by more than approximately 5 MeV, the  $d\sigma^I/(dp_n dM_{NK}^2)$  and  $d\sigma^S/(dp_n dM_{NK}^2)$  cross sections are negligibly small. The resulting  $d\sigma/(dp_n dM_{NK}^2)$  is a smooth function of  $M_{nK}$ , see Fig. 4 of Ref. [11]. When  $M_{nK}$  is close to the expected  $\Theta^+$  peak,  $|M_{nK} - M_\Theta| \leq 1 - 5$  MeV, one expects a very narrow peak, whose magnitude depends on  $p_n$  and does not depend on  $\Gamma_\Theta$ .

Next we discuss the  $p_n$ -dependence of  $d\sigma/(dp_n dM_{NK}^2)$  in the vicinity of the  $\Theta^+$  peak. The background, interference and signal cross section have very distinct  $p_n$ -dependencies, which are determined by the corresponding nuclear suppression factors. The background cross section is the largest of three in magnitude at small  $p_n$ , but it rapidly decreases with increasing  $p_n$  due to the  $|\psi_D(p_n)|^2$  factor. The interference cross section is smaller in magnitude than the background cross section because of the small value of  $\Gamma_\Theta$ , but its decrease with increasing  $p_n$  is not so steep, which is roughly determined by the  $\psi_D(p_n)$  factor in  $S(t, p_n)$ . The signal cross section is the smallest of three in magnitude, but this smallness is compensated by the slow  $p_n$ -dependence.

At small values of the final neutron momenta,  $p_n \leq 0.05$  GeV, the background dominates the cross section and one does not expect any resonance structures over the smooth background. As  $p_n$  increases,  $0.1 \leq p_n \leq 0.2 - 0.3$  GeV, the interference cross section becomes sizable, which results in a very narrow negative peak superimposed on the smooth background. As  $p_n$  is increased further,  $p_n \geq 0.3 - 0.4$  GeV, the signal cross section exceeds the background and the interference cross sections, which results in a prominent peak over the background.

This behavior is demonstrated in Fig. 3, where we plot the double differential cross section  $d\sigma/(dp_n dM_{NK}^2)$  as a function of  $M_{NK}^2$  at different values of  $p_n$ . The energy of the photon beam is  $E_\gamma = 1.2$  GeV, where the elementary  $\gamma + N \rightarrow \Lambda + K$  cross section passes through its maximum. In order to examine the dependence on the total width of the  $\Theta^+$ , we performed calculation with  $\Gamma_\Theta = 1$  MeV (left column) and  $\Gamma_\Theta = 5$  MeV (right column). The solid

curves represent the background cross section  $d\sigma^{\text{BG}}/(dp_n dM_{NK}^2)$ ; the crosses represent the full cross section  $d\sigma/(dp_n dM_{NK}^2)$ .

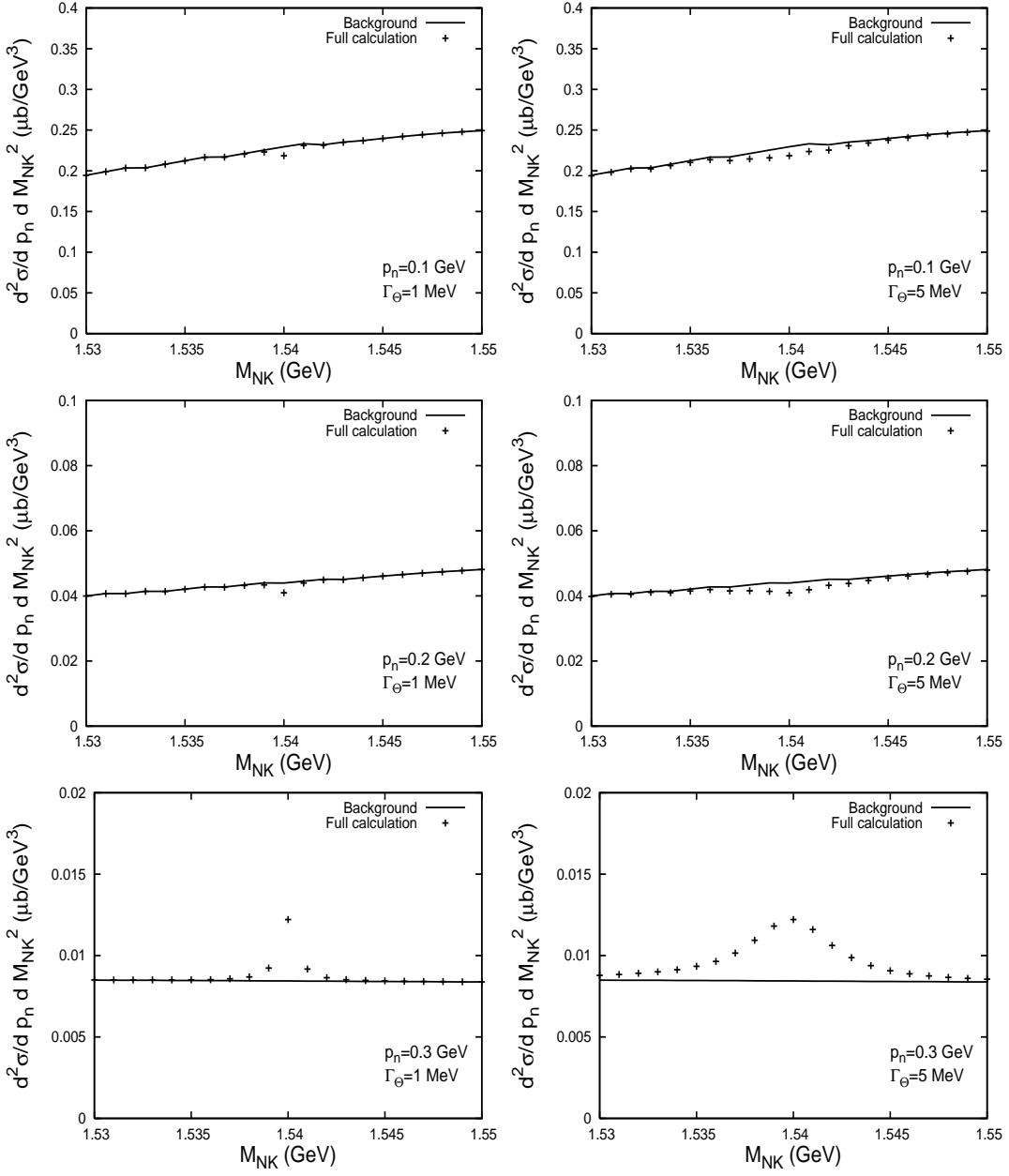


FIG. 3: The  $d^2\sigma/(dp_n dM_{NK}^2)$  cross section of the  $\gamma + D \rightarrow \Lambda + n + K^+$  reaction at  $E_\gamma = 1.2$  GeV. The solid curves is the background contribution; the crosses is the full result.

Figure 3 clearly depicts the interplay between the background, interference and signal cross sections described above. Note that as follows from Eq. (15), the height of the  $\Theta^+$  signal does not depend on  $\Gamma_\Theta$ .

The combinations of the elementary  $\gamma + N \rightarrow \Lambda + K$  cross sections (16) depend on the photon energy. Figure 4 presents our predictions for the  $d\sigma/(dp_n dM_{NK}^2)$  cross section calculated with  $E_\gamma = 1.6$  GeV. Our results presented in Figs. 3 and 4 are rather similar for  $p_n = 0.1$  GeV and  $p_n = 0.2$ . However, at  $E_\gamma = 1.6$  GeV and  $p_n = 0.3$  GeV, as a consequence of the cancellation between the  $\mathcal{A}^p$  and  $\mathcal{A}^n$  amplitudes, the interference cross section is still larger than the signal cross section. For larger  $p_n$ ,  $p_n \geq 0.4$  GeV, the signal cross section will win over the interference cross section and one will observe a distinct peak, similarly to the lower panels of Fig.3.

The size of the  $\Theta^+$  signal (the deviation of the crosses from the smooth background) depends on the photon energy  $E_\gamma$ . At  $E_\gamma = 1.2$  GeV, the deviation is 5-7% for  $p_n = 0.1 - 0.2$  GeV and rapidly becomes as large as 45% at  $p_n = 0.3$  GeV. At  $E_\gamma = 1.6$  GeV, the deviation is 7% at  $p_n = 0.1$  GeV, 27% – at  $p_n = 0.2$  GeV, and it is 12% at  $p_n = 0.3$  GeV.

While the numbers for the  $\Theta^+$  signal look impressive, the following analysis will demonstrate that if the  $\gamma + D \rightarrow \Lambda + n + K^+$  differential cross section is integrated over  $t$ ,  $p_n$  and  $E_\gamma$  as was done in the CLAS analysis [11], the  $\Theta^+$  signal disappears, mostly as a result of the cancellation between the interference and the signal contributions.

In detail, in order to compare our predictions to the CLAS result [11], we integrate the  $\gamma + D \rightarrow \Lambda + n + K^+$  differential cross section of Eqs. (14) and (15) over  $t$  and  $p_n$ . In order to simulate the lack of the forward acceptance of the CLAS detector, the minimal value of  $t$  in the integration over  $t$  is set by the cut on the  $\Lambda$  scattering angle,  $\cos\theta_\Lambda \leq 0.9$ . The integration over the final neutron momentum  $p_n$  is performed in the intervals  $0 \leq p_n \leq 0.6$  GeV and  $0.2 \leq p_n \leq 0.6$  GeV. The upper limit of integration is chosen somewhat arbitrary, with the aim to reduce the sensitivity of our results to the poorly known high-momentum tail of the deuteron wave function and to possible relativistic corrections. Since we are mostly interested in the height of the  $\Theta^+$  signal and not in its shape, this calculation is performed with  $\Gamma_\Theta = 1$  MeV.

Our results for two photon energies,  $E_\gamma = 1.2$  GeV and  $E_\gamma = 1.6$  GeV, are presented in Fig. 5. The upper panels correspond to the integration over the  $0 \leq p_n \leq 0.6$  GeV interval; the lower panels correspond to the  $0.2 \leq p_n \leq 0.6$  GeV interval. The solid curves represent the background contribution; the crosses give the results of the full calculation. One should not change the scale from  $\mu\text{b}$  in Fig. 3 and 4 to  $\text{nb}$  in Fig. 5, which is responsible for the non-smooth curves in the latter figure.

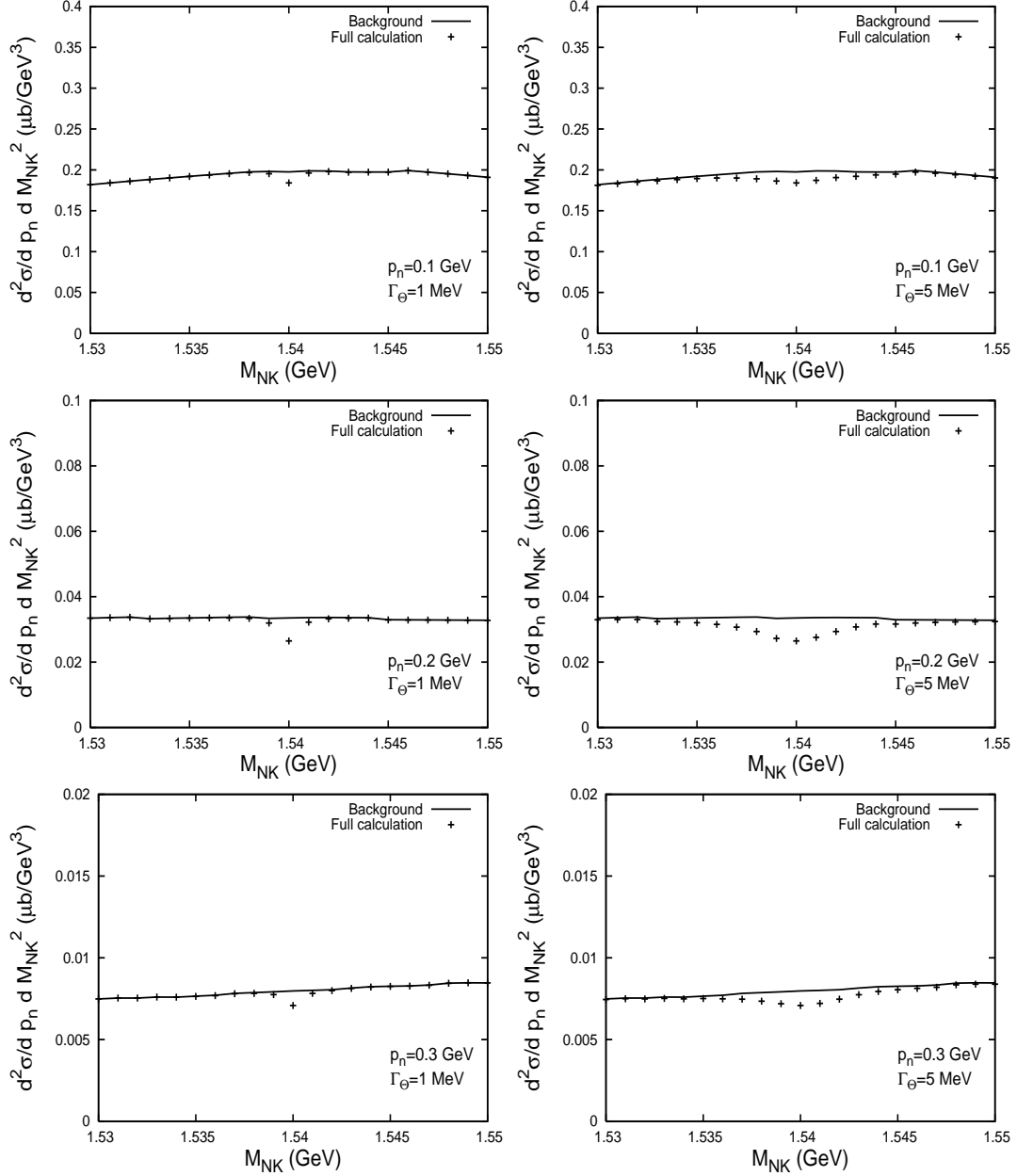


FIG. 4: The  $d^2\sigma/(dp_n dM_{NK}^2)$  cross section of the  $\gamma + D \rightarrow \Lambda + n + K^+$  reaction at  $E_\gamma = 1.6$  GeV. The solid curves is the background contribution; the crosses is the full result.

Two features of Fig. 5 deserve a discussion. First, the results of the calculations with  $E_\gamma = 1.2$  GeV and  $E_\gamma = 1.6$  GeV are fairly different. This is a consequence of the  $E_\gamma$ -dependence of the elementary  $\gamma + N \rightarrow \Lambda + K$  amplitudes. Second, the cut on the minimal value of the final neutron momentum [10] is intended in order to enhance the  $\Theta^+$  signal. Indeed, a comparison between the upper left and lower left panels shows that a tiny negative

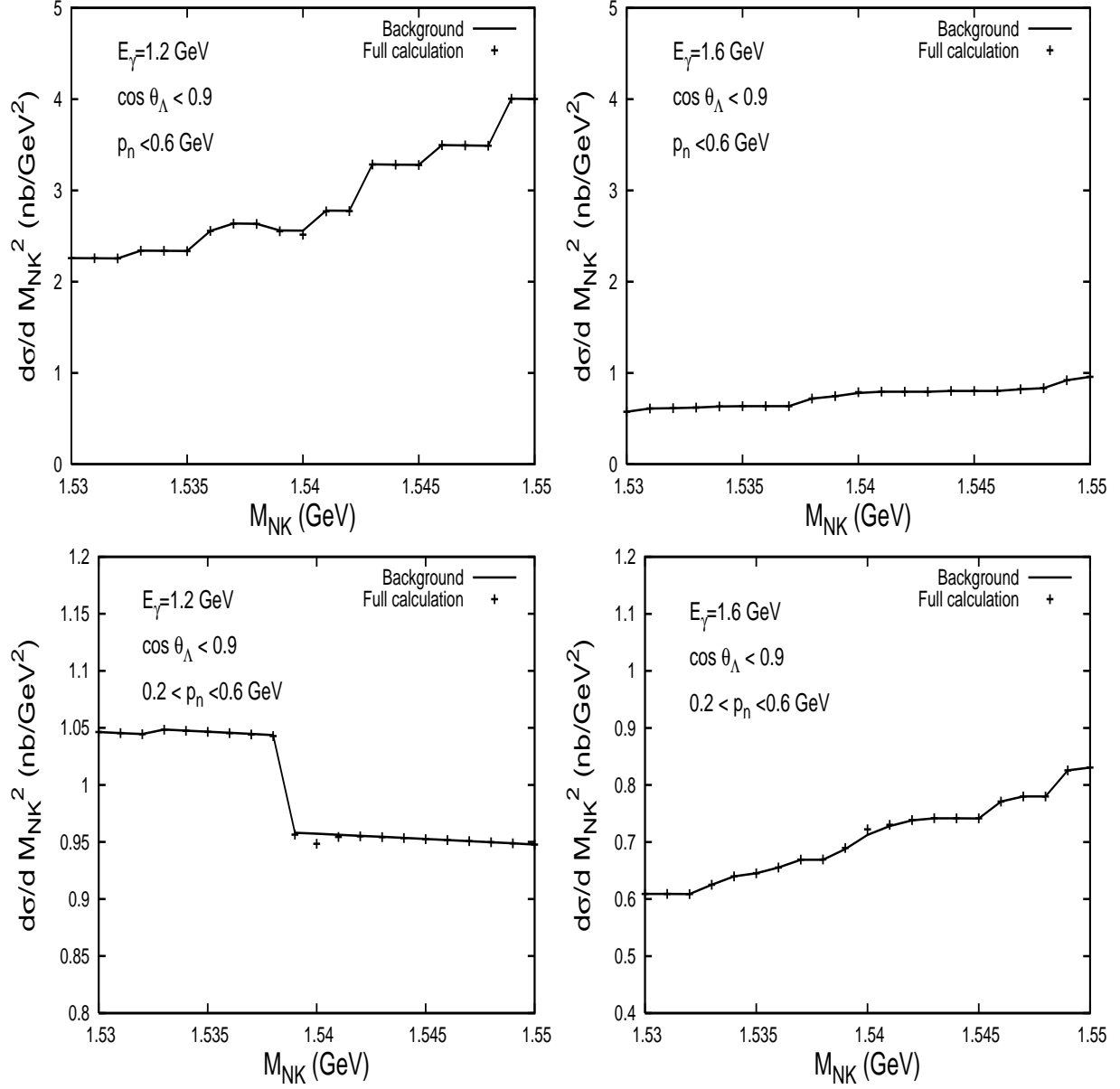


FIG. 5: The  $d\sigma/dM_{NK}^2$  cross section of the  $\gamma + D \rightarrow \Lambda + n + K^+$  reaction at  $E_\gamma = 1.2$  GeV and  $E_\gamma = 1.6$  GeV. The solid curves is the background contribution; the crosses is the full result. The calculation uses  $\Gamma_\Theta = 1$  MeV.

peak at  $M_{nK} = 1.540$  GeV appears. The deviation of the peak from the background is only 2%. Similarly for  $E_\gamma = 1.6$  GeV, a comparison between the upper right and lower right panels shows that a tiny 1% positive peak appears. Clearly, it is impossible to experimentally observe such tiny deviations from the background.

In summary, while the cut on the minimal value of the final neutron momentum indeed

enhances the  $\Theta^+$  signal, the cancellation between the interference and signal contributions in the process of integration over  $p_n$  completely washes out the desired  $\Theta^+$  signal. It appears that the  $\Theta^+$  signal from the  $\gamma + D \rightarrow \Lambda + n + K^+$  cross section can be successfully extracted only if tighter cuts on  $p_n$  and  $t$  are imposed, see examples in Ref. [10] and Figs. 3 and 4 of this work.

### III. CONCLUSIONS AND DISCUSSION

We extended our original analysis of the  $\Theta^+$  production in the  $\gamma + D \rightarrow \Lambda + n + K^+$  reaction [10] in order to provide a better comparison to the recent CLAS measurement [11]. We studied the dependence of the  $\gamma + D \rightarrow \Lambda + n + K^+$  differential cross section on the  $nK^+$  invariant mass and on the momentum of the final neutron,  $p_n$ . We demonstrated the important role of the interference between the signal and background contributions to the  $\gamma + D \rightarrow \Lambda + n + K^+$  amplitude and examined the  $p_n$ -dependence of the resulting signal, interference and background cross sections. This allowed us to identify kinematic conditions providing the enhanced sensitivity to the  $\Theta^+$  signal.

We attempted to perform a realistic comparison to the results of the CLAS measurement [11] by integrating the  $\gamma + D \rightarrow \Lambda + n + K^+$  differential cross section over  $t$  and  $p_n$ . The particular choice of cuts implemented in the integration over  $t$  and  $p_n$  consists the main source of theoretical uncertainty of the results presented in Fig. 5. We showed that as a result of the cancellation between the interference and signal contributions, the  $\Theta^+$  signal almost completely washes out after the integration over  $p_n$ , even when the  $p_n > 0.2$  GeV cut is imposed. This is consistent with the CLAS conclusion that no statistically significant structures were observed [11].

Therefore, there is no disagreement between the theory and the experiment and the CLAS result does not refute the existence of the  $\Theta^+$ .

It appears that the  $\Theta^+$  signal from the  $\gamma + D \rightarrow \Lambda + n + K^+$  cross section can be successfully extracted only if tighter cuts on  $p_n$  and  $t$  are imposed, see Figs. 3 and 4. In this respect, it seems interesting to analyse further the small deviation from the smooth background near  $M_{nK} \approx 1.53$  GeV seen in the lower panel of Fig. 4 of the CLAS publication [11].

## Acknowledgments

We thank M. Polyakov for noticing the incorrect sign of the interference cross section in our original publication [10] and for stimulating the present research.

- 
- [1] T. Nakano *et al.* [LEPS Collaboration], Phys. Rev. Lett. **91** (2003) 012002 [arXiv:hep-ex/0301020].
  - [2] K. H. Hicks, Prog. Part. Nucl. Phys. **55** (2005) 647 [arXiv:hep-ex/0504027].
  - [3] V. V. Barmin *et al.* [DIANA Collaboration], arXiv:hep-ex/0603017.
  - [4] D. Diakonov, V. Petrov and M. V. Polyakov, Z. Phys. A **359** (1997) 305 [arXiv:hep-ph/9703373].
  - [5] D. Diakonov and V. Petrov, Phys. Rev. D **72** (2005) 074009 [arXiv:hep-ph/0505201].
  - [6] C. Lorce, arXiv:hep-ph/0603231.
  - [7] R. A. Arndt, I. I. Strakovsky and R. L. Workman, Phys. Rev. C **68** (2003) 042201 [Erratum-*ibid.* C **69** (2004) 019901] [arXiv:nucl-th/0308012].
  - [8] R. N. Cahn and G. H. Trilling, Phys. Rev. D **69** (2004) 011501 [arXiv:hep-ph/0311245].
  - [9] A. Sibirtsev, J. Haidenbauer, S. Krewald and U. G. Meissner, Phys. Lett. B **599** (2004) 230 [arXiv:hep-ph/0405099].
  - [10] V. Guzey, Phys. Rev. C **69** (2004) 065203 [arXiv:hep-ph/0402060].
  - [11] S. Niccolai *et al.* [CLAS Collaboration], arXiv:hep-ex/0604047.
  - [12] MAID 2000 database, <http://www.kph.uni-mainz.de>. Kaon-MAID model is based on F.X. Lee, T. Mart, C. Bennhold, H. Haberzettl, L.E. Wright, Nucl. Phys. A **695** (2001) 237 [nucl-th/9907119] and T. Mart and C. Bennhold, Phys. Rev. C **61** (2000) 012201 [nucl-th/9906096].
  - [13] M. Lacombe, B. Loiseau, R. Vinh Mau, J. Cote, P. Pires and R. de Tournreil, Phys. Lett. B **101** (1981) 139.
  - [14] J. M. Laget, arXiv:nucl-th/0603009.
  - [15] E. Byckling and K. Kajantie, *Particle kinematics*, John Wiley & Sons, 1973, p. 118.